Available online at www.sciencedirect.com
ScienceDirect
Acta Materialia 55 (2007) 6481–6488
Acta MATERIALIA
www.elsevier.com/locate/actamat

A constrained domain-switching model for polycrystalline ferroelectric ceramics. Part II: Combined switching and application to rhombohedral materials

F.X. Li, R.K.N.D. Rajapakse *

Department of Mechanical Engineering, The University of British Columbia, 6250 Applied Science Lane, Vancouver, Canada V6T 1Z4

Received 24 July 2007; accepted 5 August 2007
Available online 21 September 2007

Abstract

A combined switching assumption (CSA) is incorporated into the constrained domain-switching model presented in part I to address the nonsymmetric deformations of ferroelectric ceramics under tension and compression. Using the CSA, the domain-switching process in rhombohedral ferroelectric/ferroelastic ceramics is analyzed in detail. The results show that in rhombohedral lead titanate zirconate (PZT) ceramics, most 109° switching can be accomplished with a minor fraction of 71° switching during electric poling, which is quite different from $BaTiO_3$ and tetragonal PZT ceramics in which only a few per cent of 90° switching can occur. Domain switching under combined uniaxial electric and mechanical tension/compression is also studied. Uniaxial tension is found to enhance electric poling while uniaxial compression inhibits it.

Keywords: Ferroelectric ceramics; Domain switching; Rhombohedral materials; Electric poling; Mechanical loading

1. Introduction

In part I of this work [1], a constrained domain-switching model for polycrystalline ferroelectric/ferroelastic ceramics was proposed and used to study domain switching in tetragonal materials. It was found that the model results based on the switching option of Berlincourt and Krueger [2] generally agree well with experiments when compared to the model results based on the switching option of Hwang el al. [3]. However, the proposed model based on that of Berlincourt and Krueger [2] still needs refinement as the nonsymmetry of simulated stress–strain curves of $BaTiO_3$ under tension and compression as shown in Fig. 1a is not as strong as that observed experimentally [4] (Fig. 1b). Nonsymmetric behaviour under tension and compression is also observed in lead titanate zirconate (PZT) ceramics [5].

It is well known that a tetragonal PZT ceramic is difficult to pole when compared to a rhombohedral PZT [6–8]. Therefore, domain-switching models suitable for tetragonal ceramics cannot be directly applied to study rhombohedral materials, and models specifically suitable for rhombohedral ceramics are desired. In addition, part I [1] focused only on pure electric or uniaxial tension (compression) loading, while in practical applications, ferroelectric ceramics are subjected to coupled electromechanical loading.

In this paper, to address the nonsymmetry of stress–strain behaviour under tension and compression, a combined switching assumption (CSA) is introduced to the constrained domain-switching model based on Berlincourt and Krueger's switching option presented in part I [1]. The validity of CSA, which assumes that two or three types of non-180° switching occur simultaneously, is discussed in Section 2. In Section 3, domain switching in rhombohedral ferroelectric/ferroelastic ceramics is analyzed by using the CSA. Section 4 presents an application of the model to

* Corresponding author. Tel.: +1 604 827 4483; fax: +1 604 822 2403.
E-mail address: rajapakse@mech.ubc.ca (R.K.N.D. Rajapakse).

1359-6454/$30.00
doi:10.1016/j.actamat.2007.08.003

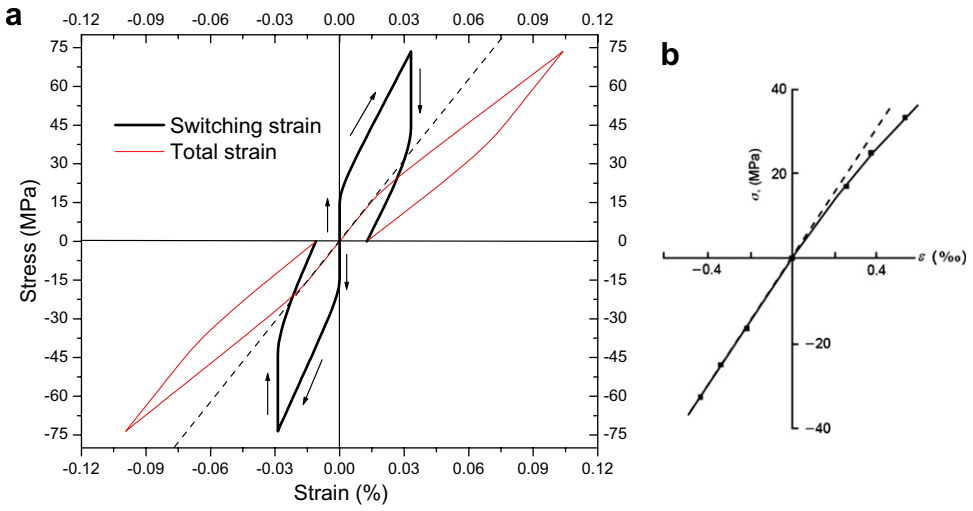

Fig. 1. Nonsymmetry of stress–strain curves of $BaTiO_3$ ceramics under uniaxial tension and compression. (a) Simulations based on unmodified model; (b) strong nonsymmetry reported by Subbarao et al. [4].

study domain switching under uniaxial electromechanical loading. A discussion of the model and conclusions are presented in Sections 5 and 6, respectively.

2. Combined switching assumption (CSA)

A useful improvement of Model B would be to allow all possible co-switching of 90° domains, such as domains 4 and 6 (Fig. 1 of Ref. [1]), to always switch together with equal fractions when an electric field is applied over the shaded area in Fig. 2. The switching process under this CSA is not complex. In fact, the CSA has a physical basis that can be explained by using a typical domain pattern in a tetragonal ferroelectric crystal (Fig. 3). In Fig. 3, equal fractions of domains 4 and 6 form a 90° domain wall along

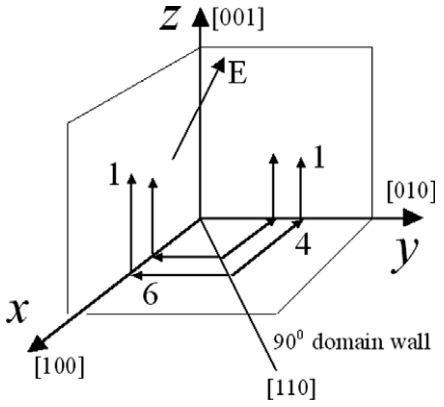

Fig. 3. Illustration of combined switching in tetragonal crystals under electric loading.

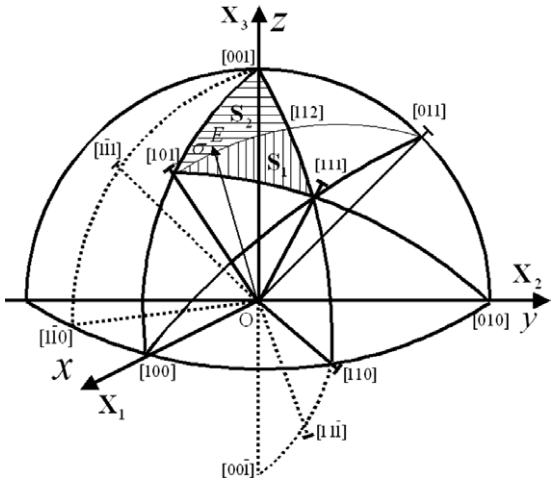

Fig. 2. Representative distribution areas of applied field in tetragonal and rhombohedral ceramics under electric loading and (or) uniaxial compression (tension) with the crystallite coordinates (x,y,z) fixed along the sample coordinates (X_1,X_2,X_3).

[1 1 0]. When an electric field is applied, domains 4 and 6 may switch to domain 1, independently or together. If they switch to domain 1 together with equal fractions, the 90° domain wall (along [1 1 0]) between them vanishes gradually after switching, and the domain wall energy is released, which may promote switching from domains 4 and 6 to domain 1.

To validate the CSA, Fig. 4 shows the polarization and strain curves of $BaTiO_3$ during electric poling with and without CSA. There is little difference between the polarization curves with and without CSA. In the case of strain, solutions corresponding to the CSA are slightly smaller than those without CSA but the remnant strains of both cases are not significantly different.

The stress–strain curves of $BaTiO_3$ ceramics under compression and tension with or without CSA are shown in Fig. 5. Similar to the electric poling case, there is only slight difference between the curves with and without CSA for tensile loading. While under compression, the switching strain with CSA is much smaller than that without CSA,

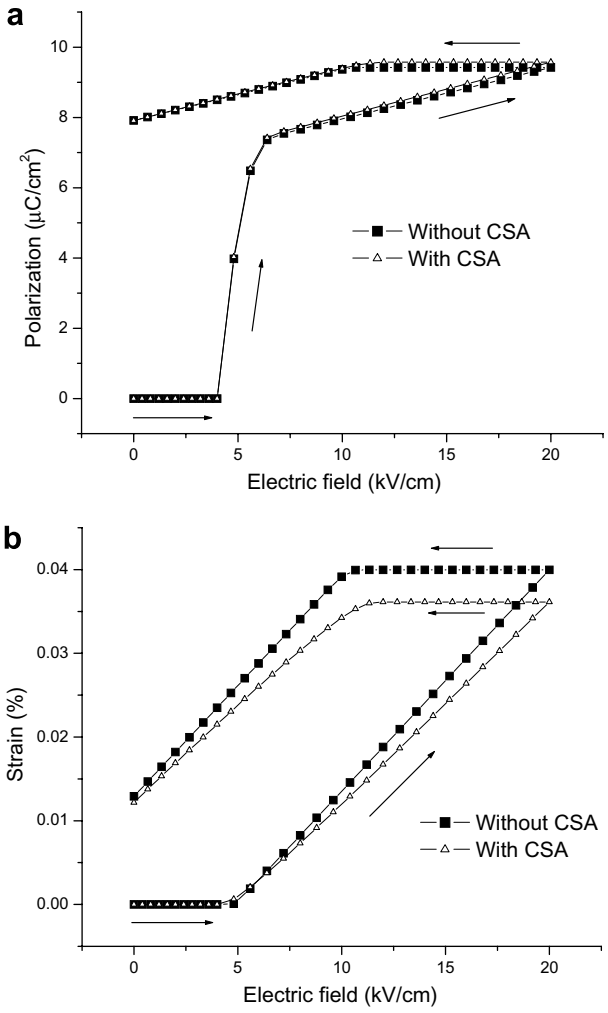

Fig. 4. Polarization and strain of $BaTiO_3$ during electric poling with and without CSA.

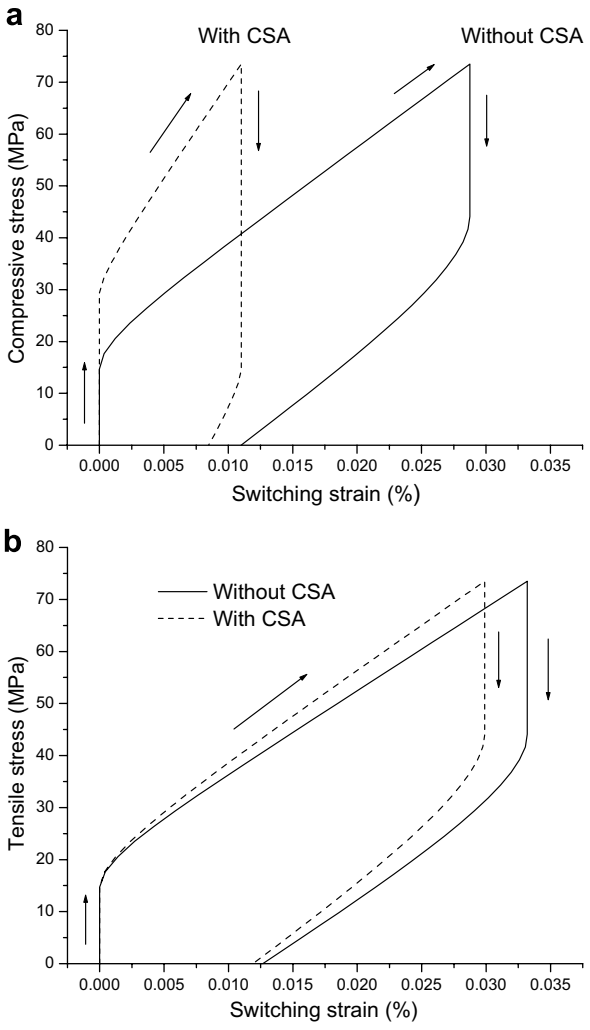

Fig. 5. Stress–strain curves of $BaTiO_3$ under compression and tension with and without CSA.

but the remnant strains are close to each other. The loading-type-dependent differences between the solutions with and without CSA can be explained. During electric poling, the activation fields for switchings 4–1 and 6–1 are close, and during tension, the activation stress for switching II–III (Fig. 5 of Ref. [1]) is closer to that for switching I–III. Therefore, the CSA does not change the activation field very much, nor does it change the switching process. However, for compression loading, the activation stress for switching I–II is normally higher than that for switching III–II. The CSA therefore implies a considerable increase in the activation stress and a decrease in the fraction of switching III–II, thus leading to a smaller strain than that without the CSA.

Using the CSA, the simulated stress–strain curves of $BaTiO_3$ ceramics under compression and tension are strongly nonsymmetric, as shown in Fig. 6. Nonlinear strains appear at a considerably lower stress under tension than that under compression, which agrees well with the experimental observations by Subbarao et al. [4] (Fig. 1b).

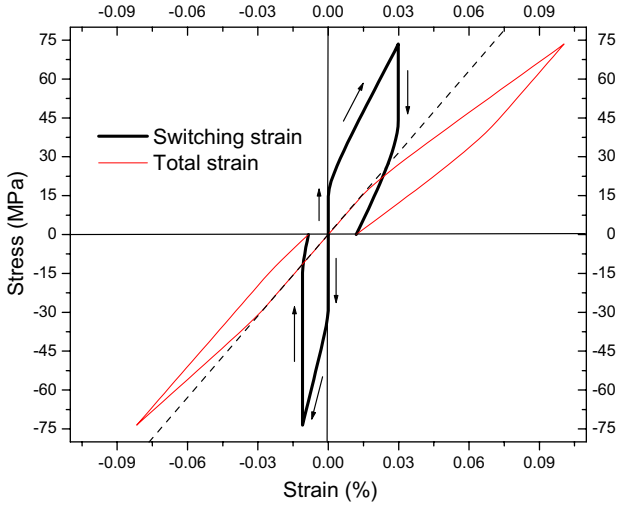

Fig. 6. Simulated stress–strain curves of $BaTiO_3$ ceramics by using CSA (dashed line denotes linear strain).

3. Application to rhombohedral polycrystalline ceramics

Noting that the present constrained domain-switching model with the CSA agrees well with experimental behavior of tetragonal ceramics under common loading cases, in this section the model is extended to rhombohedral ferroelectric/ferroelastic ceramics.

3.1. Ferroelectric case

A rhombohedral ferroelectric crystal has eight allowable polarization directions and four elongation directions. A polarization vector as shown in Fig. 7 can denote each of the eight types of domains. The spontaneous polarization vectors and strain tensors of the eight types of domains are:

$$\begin{aligned}&\mathbf{P}^{(1)}=-\mathbf{P}^{(2)}=\frac{P_0}{\sqrt{3}}(1,1,1)^{\mathbf{T}},\quad \mathbf{P}^{(3)}=-\mathbf{P}^{(4)}=\frac{P_0}{\sqrt{3}}(1,-1,1)^{\mathbf{T}},\\&\mathbf{P}^{(5)}=-\mathbf{P}^{(6)}=\frac{P_0}{\sqrt{3}}(-1,1,1)^{\mathbf{T}},\quad \mathbf{P}^{(7)}=-\mathbf{P}^{(8)}=\frac{P_0}{\sqrt{3}}(1,1,-1)^{\mathbf{T}}\end{aligned} \tag{1}$$

$$\begin{aligned}&\boldsymbol{\varepsilon}^{(1)}=\boldsymbol{\varepsilon}^{(2)}=\frac{S_0}{3}\begin{bmatrix}0&1&1\\&0&1\\\text{sym}&&0\end{bmatrix},\quad \boldsymbol{\varepsilon}^{(3)}=\boldsymbol{\varepsilon}^{(4)}=\frac{S_0}{3}\begin{bmatrix}0&-1&1\\&0&-1\\\text{sym}&&0\end{bmatrix}\\&\boldsymbol{\varepsilon}^{(5)}=\boldsymbol{\varepsilon}^{(6)}=\frac{S_0}{3}\begin{bmatrix}0&-1&-1\\&0&1\\\text{sym}&&0\end{bmatrix},\quad \boldsymbol{\varepsilon}^{(7)}=\boldsymbol{\varepsilon}^{(8)}=\frac{S_0}{3}\begin{bmatrix}0&1&-1\\&0&-1\\\text{sym}&&0\end{bmatrix}.\end{aligned} \tag{2}$$

It should be noted that in rhombohedral crystals, unlike the tetragonal case, the single-crystal deformation S_0 is not the lattice deformation ($S_{\text{lattice}}=d_{[111]}/d_{[11\bar{1}]}-1$) but is given by [9]:

$$S_0=(9/8)S_{\text{lattice}}. \tag{3}$$

Consider first the domain-switching process in an unpoled rhombohedral ferroelectric ceramic during electric poling. The analysis is conducted based on the inverse-pole-figure method used in Ref. [1] by fixing the crystallite coordinates and making the field direction vary. Fig. 2 shows the relevant representative field distribution area for both tetragonal and rhombohedral ceramics. For rhombohedral materials, the shaded area in Fig. 2 should be divided into two parts (S_1 and S_2). The boundary curve is represented by $x+y=z$, where $x=\sin\theta\cos\varphi$, $y=\sin\theta\sin\varphi$, $z=\cos\theta(x,y,z\geqslant 0)$. Based on the CSA, when an electric field is applied within S_1, i.e. $x+y>z$, the domains 4, 6 and 8 switch together to domain 1 via 109° switching. After that, domains 3, 5 and 7 switch together to domain 1 via 71° switching. When an electric field is applied within S_2, i.e. $x+y<z$, domains 4, 6 and 7 first switch together to domain 1 via 109° switching. After that, domains 3, 5 and 8 switch together to domain 1 via 71° switching. Assuming that the switching barriers for 109° and 71° are the same as that for 90° switching, i.e. $W^E_{109}=W^E_{71}=\sqrt{2}P_0E_{\text{C}}$, the combined switching criterion for 109° switching in S_1 is:

$$\begin{aligned}&4EP_0(x+y+z)/\sqrt{3}-2\mu\frac{7-5v}{15(1-v)}\cdot\frac{8S_0^2}{9}\cdot 12f_{4,6,8-1}\\&\quad=3\sqrt{2}P_0E_{\text{C}},\end{aligned} \tag{4}$$

where $f_{4,6,8-1}$ is the equal fraction of domain switching from 4 (or 6, or 8) to 1.

Divide both sides of Eq. (4) by P_0 and introduce an equivalent resisting field, $E_{\text{b}}=2\mu\frac{7-5v}{15(1-v)}\cdot\frac{8S_0^2}{9P_0}$.

Eq. (4) can be simplified to:

$$4E(x+y+z)/\sqrt{3}-E_{\text{b}}\cdot 12f_{4,6,8-1}=3\sqrt{2}E_{\text{C}}. \tag{5}$$

Similarly, the 109° switching criterion in S_2 is:

$$2E(3z+x+y)/\sqrt{3}-E_{\text{b}}\cdot 12f_{4,6,7-1}=3\sqrt{2}E_{\text{C}}. \tag{6}$$

Only after 109° switching is complete can 71° switching activate. Therefore, the 71° switching criterion in S_1 is:

$$2E(x+y+z)/\sqrt{3}-E_{\text{b}}\cdot 12(1/8+f_{3,5,7-1})=3\sqrt{2}E_{\text{C}} \tag{7}$$

and for S_2:

$$E(3z+x+y)/\sqrt{3}-E_{\text{b}}\cdot 12(1/8+f_{3,5,8-1})=3\sqrt{2}E_{\text{C}}. \tag{8}$$

For both S_1 and S_2, the 180° switching criterion is:

$$E(x+y+z)/\sqrt{3}\geqslant E_{\text{C}}. \tag{9}$$

Similar to the tetragonal case, the switching-induced polarization and strain can be expressed as:

$$\begin{aligned}P(E)=\frac{48}{4\pi}\cdot\frac{P_0}{\sqrt{3}}\Bigg[&\int_{S_1}\int 2(x+y+z)(2f_{4,6,8-1}+f_{3,5,7-1})\sin\theta\,\mathrm{d}\theta\,\mathrm{d}\varphi\\&+\int_{S_2}\int(x+y+3z)(2f_{4,6,7-1}+f_{3,5,8-1})\sin\theta\,\mathrm{d}\theta\,\mathrm{d}\varphi\\&+\int_{S_1+S_2}\int 2(x+y+z)f_{2-1}\sin\theta\,\mathrm{d}\theta\,\mathrm{d}\varphi\Bigg]\end{aligned} \tag{10}$$

$$\begin{aligned}\varepsilon(E)=\frac{48}{4\pi}\cdot\frac{8}{3}S_0\Bigg[&\int_{S_1}\int(xy+yz+zx)(f_{4,6,8-1}+f_{3,5,7-1})\sin\theta\,\mathrm{d}\theta\,\mathrm{d}\varphi\\&+\int_{S_2}\int(xy+yz+zx)(f_{4,6,7-1}+f_{3,5,8-1})\sin\theta\,\mathrm{d}\theta\,\mathrm{d}\varphi\Bigg].\end{aligned} \tag{11}$$

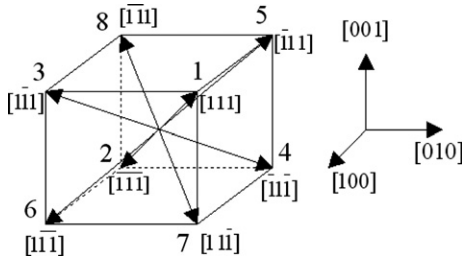

Fig. 7. Illustration of eight types of domain in rhombohedral crystals.

3.2. Ferroelastic case

In ferroelastic rhombohedral crystals, there are only four types of domains with their elongation axes along [111], [1$\bar{1}$1], [$\bar{1}$11] and [11$\bar{1}$]. It is convenient to redefine

the domain types in Fig. 7 by turning domains 1 and 2 to domain I; domains 3 and 4 to domain II; domains 5 and 6 to domain III; and domains 7 and 8 to domain IV. It should be noted that in rhombohedral ferroelastic crystals, only 71° domain switching is induced by stress.

During uniaxial compression loading with the CSA, by fixing the crystallite coordinates and making the compression direction vary on the shaded area in Fig. 2, 71° switchings I–IV, II–IV and III–IV occur at the equal fraction $f_{\mathrm{I,II,III–IV}}$. The switching criterion for co-switching from I, II, III to IV is:

$$\frac{8}{3}\sigma S_0(xz+yz-xy)-2\mu\frac{7-5v}{15(1-v)}\cdot\frac{8S_0^2}{9}\cdot 12 f_{\mathrm{I,II,III–IV}} = 3W_{71}^{\sigma}, \tag{12}$$

where the energy barrier for 71° switching is set to, $W_{71}^{\sigma}=\sigma_{\mathrm{C}}S_{\mathrm{lattice}}=(8/9)\sigma_{\mathrm{C}}S_0$ to activate domain switching at the coercive stress.

By dividing both sides of Eq. (12) by $S_{\mathrm{lattice}}=(8/9)S_0$ and introducing the back stress, $\sigma_{\mathrm{b}}=2\mu\frac{7-5v}{15(1-v)}S_0$, Eq. (12) reduces to:

$$3\sigma(xz+yz-xy)-12\sigma_{\mathrm{b}}f_{\mathrm{I,II,III–IV}}=3\sigma_{\mathrm{C}}. \tag{13}$$

Domains II, III and IV switch together to domain I during tension loading based on the CSA. The analysis under tension is similar to that under compression and is not repeated here.

3.3. Numerical results

The rhombohedral ceramic used in the simulation is PZT-60/40 [7,8,10]. The materials constants are listed in Table 1. The calculated back electric field is $E_{\mathrm{b}}=28.6$ kV/cm, back stress $\sigma_{\mathrm{b}}=229$ MPa and coercive stress $\sigma_{\mathrm{C}}=\sqrt{2}P_0E_{\mathrm{C}}/S_{\mathrm{lattice}}=95$ MPa. For comparison, the material constants of tetragonal PZT-45/55 [7,8,10] are also listed in Table 1 and are used in Section 4 for uniaxial electromechanical loading.

As there are no single-domain PZT crystals reported in the literature, the magnitude of spontaneous polarization, P_0, for single-domain PZT is strictly unknown. Berlincourt and Krueger [2] measured the longitudinal strain of tetragonal PZT after poling and estimated the fraction of 90° domain switching to be about 44%. By measuring the remnant polarization $P_{\mathrm{r}}=39\ \mu\mathrm{C/cm^2}$ and assuming complete 180° switching, they estimated P_0 for single-domain PZT as 75 $\mu\mathrm{C/cm^2}$. Based on Li and Rajapakse [1], it is very likely that bulk of the 44% of 90° switching occurred from domains 4 and 6 to domain 1 (referring to Fig. 1 of Ref. [1]) as it is superior to switching from domains 3 and 5 to domain 1. If so, Berlincourt and Krueger probably underestimated the remnant polarization considerably and thus overestimated P_0 for single-domain PZT.

Table 1
Material constants of rhombohedral PZT-60/40 and tetragonal PZT-45/55 ceramics

Material constants	Rhombohedral PZT	Tetragonal PZT
Shear modulus G (10^9 N m^{-2})	30	35
Poisson's ratio v	0.3	
Spontaneous polarization P_0 (μC cm^{-2})	52	
Lattice deformation S_{lattice}	0.65%	2.77%
Single-crystal deformation S_0	0.73%	2.77%
Coercive field E_{C} (kV cm^{-1})	8.4	17

In this paper, P_0 is estimated from the maximum remnant polarization, 48 $\mu\mathrm{C/cm^2}$, for PZT ceramics near the morphotropic phase boundary (MPB), where tetragonal and rhombohedral phases coexist [6]. Assuming that both 180° and non-180° switchings are complete in morphortropic PZT ceramics [8], the maximum achievable remnant polarization can be estimated by [11]:

$$P_{\max}^{r}\approx(1-1/n)P_0, \tag{14}$$

where n is the number of equivalent polar directions in PZT ceramics near MPB and $n=6+8=14$.

Fig. 8 shows the polarization and strain curves of rhombohdral PZT-60/40 during electric poling by using the CSA. It is significantly different from the tetragonal case where only a few per cent of 90° switching is accomplished at $5E_{\mathrm{C}}$. In rhombohedral PZT ceramics, complete 109° domain switching can be accomplished when the poling field reaches $2.6E_{\mathrm{C}}$ (22 kV cm^{-1}). Thereafter, domain switching saturates until the field is about 40 kV cm^{-1} (4.8 E_{C}) and 71° domain switching starts. In practical situations, the poling field is usually lower than 40 kV cm^{-1}, and therefore the chances of 71° domain switching during poling is not high. On removing the poling field, the remnant polarization is 32 $\mu\mathrm{C\ cm^{-2}}$ and the remnant strain is 0.13%, which are closer to the experimental results of 35 $\mu\mathrm{C\ cm^{-2}}$ and 0.16%, respectively [7,12].

Fig. 9 shows the stress–strains curves of PZT-60/40 ceramics under tension and compression with the CSA. Similar to the results of tetragonal ceramics in Fig. 6, the switching strain in rhombohedral ceramics under tension is much larger than that under compression. Li et al. [8] and Rogan [10] reported that rhombohedral PZT-60/40 exhibits nearly linear strain up to 200 MPa in compression. The simulated total strain is plotted in Fig. 9 because in experiments only total strain can be measured. The results show that during compression loading with the CSA, the switching strain appears at about 190 MPa and is less than 8% of the total strain up to 280 MPa, which agrees well with the experimental results [8,10].

4. Domain switching under combined uniaxial electromechanical loading

The above numerical results and those in Ref. [1] are restricted to domain switching under pure electric or uniaxial tension (compression) loading. Theoretically, the proposed constrained domain-switching model can also be used under general electromechanical loading. The

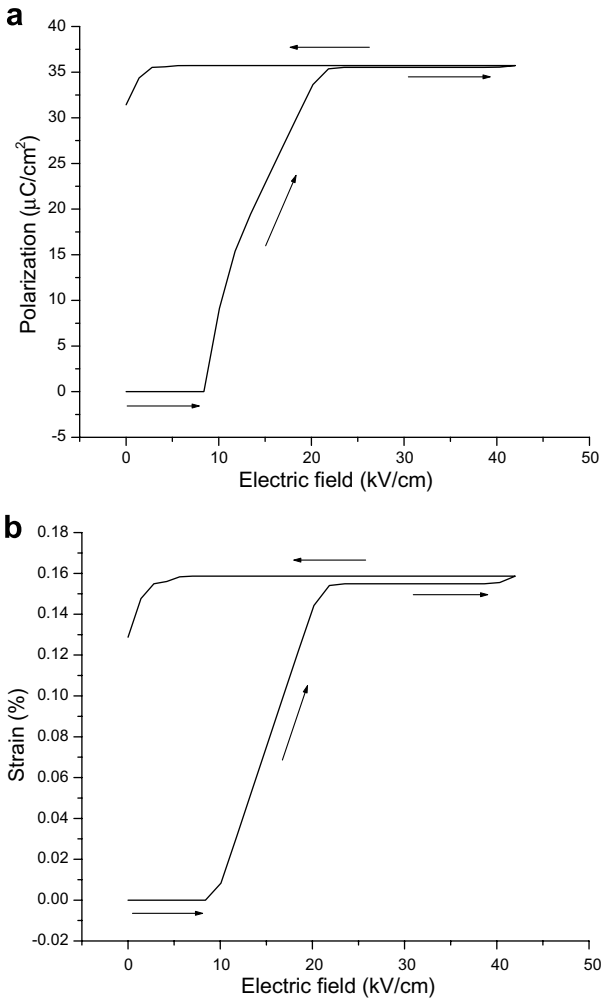

Fig. 8. Polarization and strain curves of rhombohedral PZT ceramics under electric poling.

application of the inverse-pole-figure method [1] to a loading case involving combined electric and tension (or compression) loading is demonstrated in this section.

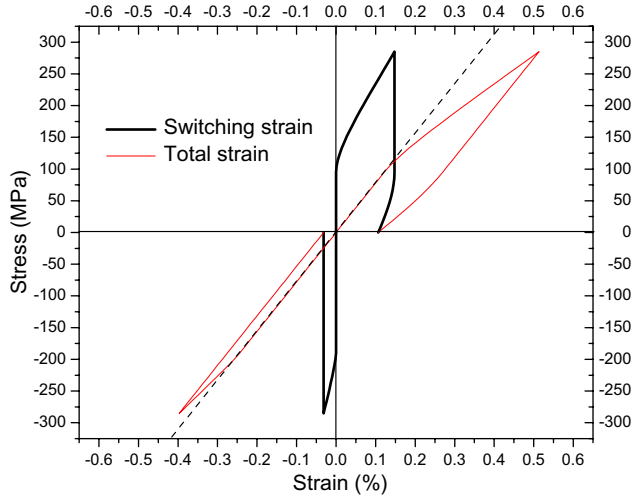

Fig. 9. Simulated stress–strain curves of rhombohedral PZT ceramics under compression and tension.

Without loss of generality, the combined uniaxial loading of tetragonal materials is considered as an example. The domain type is defined in Fig. 1 of Ref. [1] and the inverse-pole-figure method requires consideration of uniaxial electromechanical loading applied only to the shaded area in Fig. 2.

Consider the case where uniaxial tension (compression) is fixed and the magnitude of electric loading is varied. The tension (compression) preload is set below the coercive stress such that no domain switching occurs unless an electric field is applied. Under the CSA, during electric loading, domains 4 and 6 switch to domain 1 with equal fractions, f_{46-11} ($\leqslant 1/6$). Upon removing the electric field, back-switching may occur from domain 1 to domains 4 and 6 with equal fractions, f_{11-46} ($\leqslant 1/6$).

Following a procedure similar to Section 3 and Ref. [1], the combined switching criterion for switching from domains 4 and 6 to domain 1 can be expressed as:

$$E(2z+x+y)+\sigma S_0/P_0\cdot(2z^2-x^2-y^2)-E_b\cdot 6f_{46-11}=2\sqrt{2}E_C, \tag{15}$$

where $E_b=2\mu\frac{7-5v}{15(1-v)}\cdot S_0^2/P_0$ is the back electric field and is same as that under pure electric loading in Ref. [1].

The combined 90° switching fraction f_{46-11} can then be obtained as a function of the applied electric field E and applied stress σ. Obviously, it can be seen from Eq. (15) that uniaxial tension reduces the activation field for 90° switching while uniaxial compression increases it.

Upon removing the electric field, the switching criterion for combined 90° back-switching from domain 1 to domains 4 and 6 is:

$$E_b\cdot 6\left(f_{46-11}^{\max}-f_{11-46}\right)-E(2z+x+y)-\sigma S_0/P_0\cdot(2z^2-x^2-y^2)=2\sqrt{2}E_C, \tag{16}$$

where $f_{46-11}^{\max}$ is the maximum achievable fraction of combined 90° switching from domains 4 and 6 to domain 1 at the maximum electric field.

The switching polarization and strain can be obtained by integration over the shaded spherical area in Fig. 2.

The application of the model is examined by considering tetragonal PZT-45/55 ceramics [7,12] with properties listed in Table 1. The shear modulus, G, for PZT-45/55 is not available in the literature [7,12] and is approximated from the corresponding modulus of PZT-40/60 [8,10], which has a very similar composition. The calculated back electric field is $E_b=541$ kV/cm.

Fig. 10 shows the switching polarization and strain curves under electric loading with a preload stress of zero, 45 MPa and −45 MPa. The maximum applied electric field is set to $3E_C$ (51 kV cm^{-1}). It can be seen from Fig. 10 that compared to the zero preload case, the coercive field for 45 MPa tension preload is slightly smaller as the tension preload reduces the activation field for 90° switching. Although a compression preload increases the activation field for 90° switching, the coercive field for the compression preload is nearly the same as the preload does not

affect 180° switching. In general, the polarization curves are not sensitive to the preload stress because most of switching polarization is due to 180° switching. As expected, the 45 MPa tension preload considerably increases both the poling strain and the remnant strain, while an equal compression preload decreases them.

Achievable fractions of 90° switching during and after electric poling with different preload stresses are shown in Table 2. A tension (compression) preload of 45 MPa enhances (reduces) the 90° switching fractions by 2.44% both during and after poling. It has been reported based on experiments that a preload compressive stress increases the coercive field and reduces the poling polarization and strain [13,14]. Recently, Kounga Njiwa et al. [15] found that radial compression can reduce the coercive field of a disk-shaped PZT ceramic and increase the remnant polarization. As domain switching is a volume-conserving process, hydrostatic pressure has little effect on domain switching [16]. Thus, as far as domain switching is concerned, radial compression is almost equivalent to an axial tension for a disk-shaped specimen. Although the experimental results relate to rhombohedral ceramics [13] or ceramics near the MPB [14,15] which differ from the tetragonal materials used in the present simulations, the present model shows good qualitative agreement with the experimental results under combined uniaxial electromechanical loading.

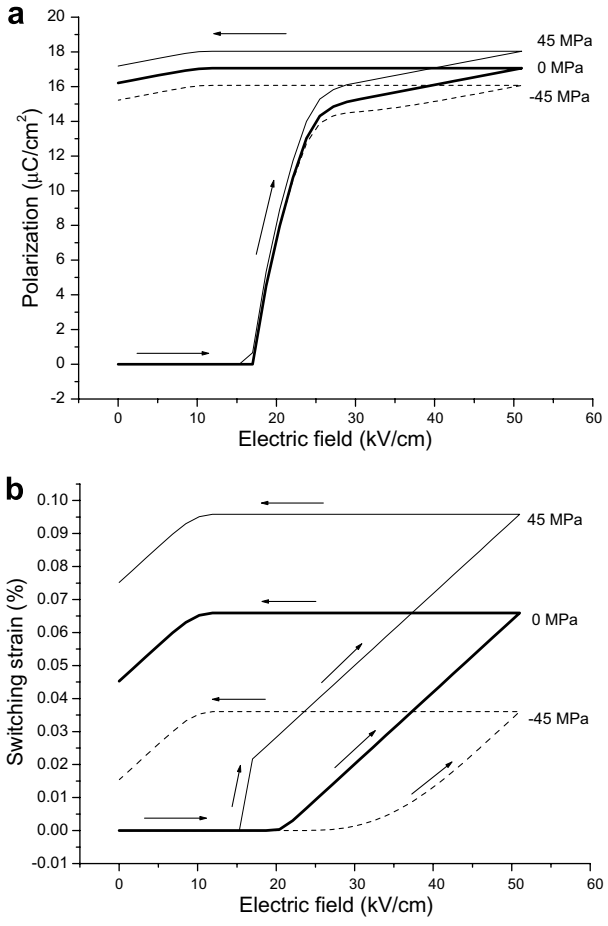

Fig. 10. Polarization and strain curves of tetragonal PZT ceramics under electric poling with different preload stress.

Table 2
Calculated fractions of 90° switching in tetragonal PZT ceramics during and after electric poling with different preload stress

Preload stress (MPa)	Fraction of 90° switching (%)	
0	At 3Ec (51 kV cm^{-1})	6.54
45		8.99
−45		4.1
0	Upon removing electric field	4.44
45		6.89
−45		2.0

5. Discussion

The present model shows that in rhombohedral PZT ceramics, 109° switching can be completed when the electric field is $2.6E_C$ (22 kV cm^{-1}), but 71° switching is very limited even at $5E_C$ (42 kV cm^{-1}). In comparison, the achievable fractions of 90° switching are only a few per cent for both $BaTiO_3$ ceramics at $5E_C$ (20 kV cm^{-1}) [1] and tetragonal PZT at $3E_C$ (51 kV cm^{-1}). The issue of the large difference in fractions of achievable non-180° domain switching between the tetragonal and rhombohedral ferroelectric ceramics deserves further attention. It is not principally due to the different crystal symmetries, but to the large difference in single-crystal deformation S_0 during the paraelectric to ferroelectric (P–F) phase transition. As discussed in Ref. [1] and shown in Section 3 of this paper, for both tetragonal and rhombohedral ceramics, during electric poling, the fraction of achievable non-180° switching is strongly dependent on the back electric field E_b, which is proportional to S_0^2/P_0. The larger the E_b is, the smaller the fraction of non-180° switching that can be achieved. The single-crystal deformation S_0 for tetragonal PZT is 2.77%, about 3.8 times that for rhombohderal PZT [7], resulting in $E_b = 541$ kV cm^{-1} vs. 28.5 kV cm^{-1} for rhombohedral PZT. Tetragonal PZT ceramics are therefore much more difficult to pole when compared to rhombohedral PZT [6–8].

From Fig. 10b and Table 2, it can be seen that the longitudinal switching strain is not exactly proportional to the fractions of 90° switching (or non-180° switching) when the latter is small. The remnant strain for 45 MPa tension preload is about 0.075%, 5 times of that for 45 MPa compression preload (0.015%), while the remnant fraction of 90° switching for the former (6.89%) is less than 3.5 times of the latter (2.0%). This is because according to the switching criterion, the initial 90° switching occurs among those domains with their original polar directions around 135° to the electric field and only induces smaller longitudinal strain. Those domains with their original polar directions around 90° to the electric field can generate larger longitudinal strains through 90° switching, but this 90° switching only occurs at a larger electric field. Therefore the use of

remnant strain to estimate the fraction of 90° switching (or 180° switching) requires careful consideration especially when the latter is relatively small (say <20%).

6. Conclusions

This paper successfully incorporates a combined switching assumption into the constrained domain-switching model presented in Ref. [1] to account for nonsymmetry of stress–strain curves. The model is then applied to analyze domain switching in rhombohedral ferroelectric/ferroelastic ceramics under electric or uniaxial tension (compression) loading. It is shown that the model can be used to study domain switching under combined uniaxial electric and mechanical electromechanical loading and the simulations show good qualitative agreement with experimental results. The major findings of the present study are: (i) Berlincourt and Krueger's switching option [2] with the CSA can reproduce existing experimental results very well, including nonsymmetric deformations in ferroelectric ceramics under compression and tension loading, which implies that combined switching may be the dominant switching process in real ceramics; and (2) the large differences in achievable fractions of non-180° domain switching between tetragonal and rhombohedral ferroelectric ceramics are mainly due to the large differences in lattice deformations during P–F phase transitions.

Acknowledgement

The work presented in this paper was supported by a grant from the Natural Sciences and Engineering Research Council of Canada (NSERC).

References

[1] Li FX, Rajapakse RKND. Acta Mater 2007;55:6472–80. doi:10.1016/j.actamat.2007.08.002.
[2] Berlincourt D, Krueger HHA. J Appl Phys 1959;30:1804.
[3] Hwang SC, Lynch CS, McMeeking RM. Acta Metall Mater 1995;43:2073.
[4] Subbarao EC, McQuarrie MC, Buessem WR. J Appl Phys 1957;28:1194.
[5] Fett T, Müler S, Munz D, Thun G. J Mater Sci Lett 1998;17:261–5.
[6] Berlincourt DA, Cmolik C, Jaffe H. Proc Inst Radio Eng 1960;48:220.
[7] Hoffmann MJ, Hammer M, Endriss A, Lupascu DC. Acta Mater 2001;49:1301.
[8] Li JY, Rogan RC, Üstündag E, Bhattacharya K. Nature Mater 2005;4:776.
[9] Uchida N, Ikeda T. Jpn J Appl Phys 1967;6:1079.
[10] Rogan RC. PhD Thesis, California Inst Technology 2004.
[11] Li FX, Fang DN, Soh AK. Scripta Mater 2006;54:1241.
[12] Lupascu DC. Fatigue in Ferroelectric Ceramics and Related Issues. Berlin/New York: Springer Verlag; 2004.
[13] Lynch CS. Acta Mater 1996;44:4137.
[14] Fang DN, Li CQ. J Mater Sci 1999;34:4001.
[15] Kounga Njiwa AB, Aulbach E, Granzow T, Rödel J. Acta Mater 2007;55:675.
[16] Jaffe B, Cook WR, Jaffe H. Piezoelectric Ceramics. London/New York: Academic Press; 1971 [p. 167].